

Luminescent amorphous alumina nanoparticles in toluene solution

W J Zhang¹, X L Wu^{1,3}, J Y Fan¹, G S Huang¹, T Qiu¹ and Pau K Chu²

¹ National Laboratory of Solid State Microstructures and Department of Physics, Nanjing University, Nanjing 210093, People's Republic of China

² Department of Physics and Materials Science, City University of Hong Kong, Kowloon, Hong Kong, People's Republic of China

E-mail: hkxluw@nju.edu.cn

Received 10 July 2006, in final form 23 September 2006

Published 13 October 2006

Online at stacks.iop.org/JPhysCM/18/9937

Abstract

We report on blue luminescence from alumina nanoparticles suspended in toluene solution. They were fabricated through ultrasonic treatment of porous anodic alumina membrane. The photoluminescence in the suspension of alumina nanoparticles shows considerable blueshift as larger particles precipitate. Transmission electron microscopy observations confirm the occurrence of the precipitation. A mixed mechanism combining the surface bonding states with widened bandgaps of alumina nanoparticles by the quantum confinement effect is presented. It agrees well with the observed photoluminescence results.

The alumina nanoparticle is one of the most important new fine ceramic materials for its excellent properties such as high melting point, low electrical conductivity, thermal and chemical stability and strong oxidation and corrosion resistance. Its application covers a wide range of fields, such as the micro-electronics industry, medical science, material engineering and so on [1–3]. Also, porous alumina has recently attracted great interest as a template for fabricating various nanostructured materials [4–11], such as carbon and Ni nanotubes, Si nanodots, CdS nanoparticles and ZnO nanowire arrays [8, 11–15]. However, little has been done on the optical properties of nanoscaled alumina particles due to the difficulty of sample preparation. Here we report fabrication of amorphous alumina nanoparticles in toluene suspension based on porous anodic alumina (PAA) membrane and investigation of their photoluminescence (PL) properties. The obtained nanoparticles show intensive blue emission that strongly depends on particle sizes and solvent chosen. A luminescence mechanism combining surface bonding states with the energy levels of alumina nanoparticles modified by the quantum confinement effect is presented, which explains well the observed luminescence spectra.

³ Author to whom any correspondence should be addressed.

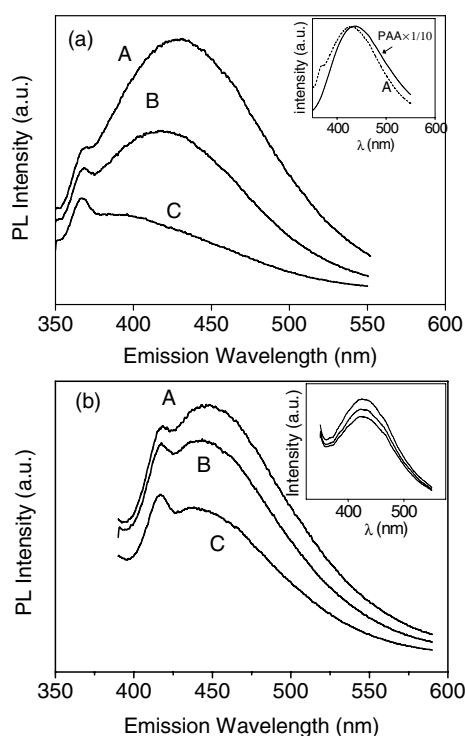


Figure 1. (a) PL spectra of samples A, B and C, taken under excitation with the 330 nm line of a Xe lamp. The inset shows the PL spectra of the PAA membrane in toluene solvent as well as sample A, taken under the same excitation. (b) PL spectra of samples A, B and C, taken under excitation with the 370 nm line of a Xe lamp. The inset shows the PL spectra of alumina powders in chloroform solvent, taken under excitation with the 330 nm line of a Xe lamp.

High-purity Al foil (99.99%) was used to fabricate the PAA membranes. Al foil was electrochemically etched in 0.5 M oxalic acid under a dc voltage of 40 V at 5 °C for 12 h. Surplus Al substrate was removed with saturated CuCl_2 aqueous solution. The achieved PPA membrane was ultrasonically treated in de-ionized water for 10 s to remove adhering Cu [16]. Then it was dried and ground in a mortar box, where alumina powder was collected. We put the powder in toluene followed by ultrasonic treatment for 1 h to achieve a homogeneous distribution of alumina particles and to further decrease the particle sizes. The obtained alumina solution right after the ultrasonic treatment was named sample A. After keeping for 2 and then 4 min, sample A becomes samples B and C, respectively. Transmission electron microscopy (TEM) observation was conducted on an FEI TECNAI G² 20 S-TWIN TEM at an accelerating voltage of 200 kV. The PL spectrum measurement was performed on a Hitachi F4040 fluorescence spectrophotometer. All measurements were made at room temperature.

Figure 1(a) shows PL spectra of samples A, B, and C, respectively, taken under excitation with the 330 nm line of a Xe lamp. The emission band of sample A is centred at 430 nm. Note that the small peak at ~365 nm is the Raman spectrum of the toluene solvent [17]. The inset shows the PL of the PAA membrane dipped in toluene excited at 330 nm. The PL curve has a maximum at 435 nm which resembles that of sample A in shape but with much larger intensity. This suggests that the PL in alumina particles may have a similar origin as that in the PAA membrane [17]. The small intensity may be caused by fewer luminescent centres in suspending

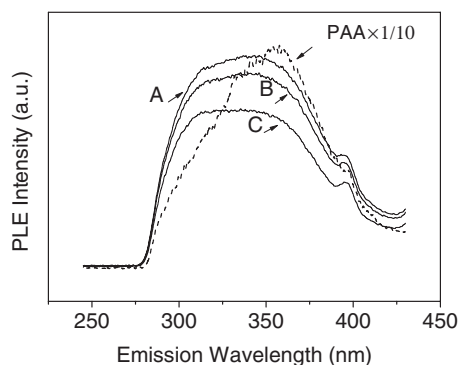


Figure 2. PLE spectra of samples A, B, C and the PAA membrane in toluene solvent, taken by monitoring at 450 nm.

alumina particles due to their much smaller volumes compared with that of PAA membrane. The PL in sample B is shifted to 418 nm. Its intensity is decreased. Sample C shows a greater blueshift; its PL peak wavelength is about 385 nm. Its emission intensity further decreases. Figure 1(b) presents the PL spectra of samples A, B, and C under lower excitation energy at 370 nm. Compared with figure 1(a), the PL shows smaller blueshift among three samples. Note that the full widths at half maximum (FWHMs) of the emission bands become smaller for lower excitation energy at 370 nm. The PL spectra of sample A were obtained right after the ultrasonic treatment, so alumina particles with all possible sizes in the solution should have contributions to the PL. When sample A was kept for 2 and 4 min, some larger particles should have precipitated; only smaller particles remain in the solution and contribute to the PL. Since no other treatments were conducted on samples B and C with respect to the freshly prepared sample A, we conclude that decreasing particle sizes may have led to the blueshifts of the PL. The inset shows the PL of alumina particles after the same treatment as mentioned above, but dispersed in chloroform solvent excited at 330 nm. It presents a similar variation in PL intensity compared to that in toluene solvent, but shows no obvious blueshift in peak position. It is clear that the toluene solvent might have great contributions to the blueshifts of the PL.

Figure 2 shows PLE spectra of samples A, B, C and the PAA membrane dipped in toluene solvent taken by monitoring at 450 nm. It can be obtained that the PL curves of samples A, B and C are at least composed of two different peaks, the peak around 360 nm, which is similar to that of the PAA membrane in toluene solvent, as well as the peak with a smaller wavelength, around 315 nm. Obviously, the peak with short wavelength has a different origin from that with the longer wavelength. With the weakening of PLE intensity, it can be obtained that the ratio of intensity of the peak with longer wavelength to that with shorter wavelength is decreased. However, no shift of the peak is observed in PLE spectra.

Figure 3(a) shows the TEM image of particles in sample A. It contains alumina particles or pieces with different dimensions. The alumina particles have sizes ranging from several to tens of nanometres. Some bulks as large as more than one hundred nanometres belong to incompletely ground pieces. There are also some short wire-like structures. They are broken PAA tubes. The upper inset in figure 3(a) shows a magnified image of one cluster which contains surplus PAA tubes with ordered pore arrays. The lower inset depicts the selected area electron diffraction (SAED) pattern of the particles. A broad halo spot indicates amorphous structure of the alumina particles [18]. Figure 3(b) shows the TEM image of suspended particles in sample C. It contains only small particles. They are 5–30 nm in diameter and

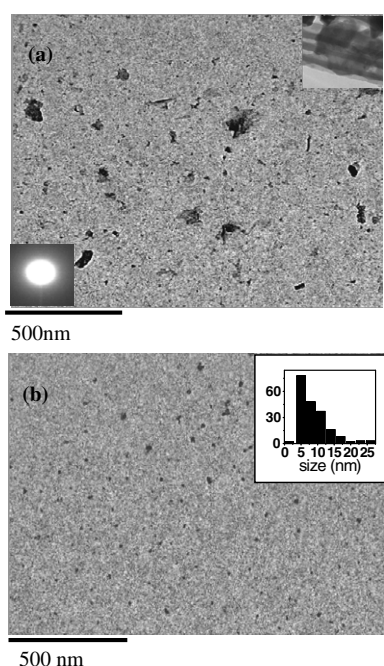


Figure 3. (a) TEM image of sample A. The upper inset shows the image of pore arrays of incompletely ground alumina particles. The lower inset gives the SAED pattern of particles in sample A. (b) TEM image of sample C. The inset shows the size distribution of alumina particles.

nearly spherical. The upper inset depicts the corresponding size distribution counted for over 200 particles. Most particles distribute in the range 5–15 nm. This result indicates that after standing for several minutes larger alumina particles precipitate, and only smaller ones remain and contribute to the emission. They have small enough sizes that the quantum confinement effect can occur and induce the blueshift of the PL.

As we knew, the PL and PLE peaks in PAA membrane are due to the optical transitions within defect energy levels by exhibiting an obvious single luminescent peak [19, 20]. However, in our experiment, the PL presents a continuous blueshift under the same excitation, while the PLE displays a wide absorption band, which is different from previous experiment results. It can be clearly seen that the physical mechanism of the luminescence in our experiment differs from the model of defect energy levels.

It is reported that several types of interactions might occur between the alumina surface and the aromatic rings [21, 22]. For toluene, owing to the electron-donating nature of the methyl group, an increased electron density of the aromatic ring may be favourable for stronger interaction with the alumina surface [23]. These might be responsible for the wide absorption band of the PLE. It is suggested that absorption may be induced by transitions in surface bonding energy levels which might be introduced from the interactions as mentioned above. These surface bonding energy levels, combined with the oxygen defect levels, illustrate well the wide absorption band in PLE. In sample A, a great number of large particles remain dispersed in the solution, so the optical absorption within oxygen defect energy levels is dominating. However, the surface bonding effect becomes more obvious owing to the large surface-to-volume ratio of small alumina particles as most large particles precipitate. So, the ratio of intensity of the peak with longer wavelength (oxygen defect energy levels) to that

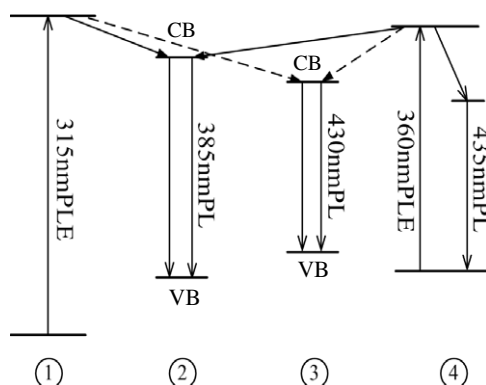


Figure 4. Schematic diagrams exhibiting optical transition process. ①–④ represents the energy levels of surface bonding structure, nanoscaled alumina (large and small) particles, and oxygen vacancy related defects, respectively.

with shorter wavelength (surface bonding energy levels) is decreased. As these two kinds of absorption bands have no correlation with the particle size, no shift of peak position is observed. For PL, however, an obvious blueshift is observed, which has a strong correlation with the particle size. So, it is suggested that the optical emission process is different from the optical absorption process. According to theoretical calculation [24], the positions of conduction and valence bands of Si change owing to the interaction between Si and toluene solvent. Therefore, the energy levels of alumina nanoparticles might be changed due to the influence of the surface bonding structure except for the quantum confinement effect. Figure 4(a) depicts the corresponding schematic diagram. The absorption process occurs in the surface bonding states and oxygen vacancy defect energy levels, as shown by ① and ④, while the optical emission takes place in modified energy levels of alumina nanoparticles (see ② for small particles and ③ for large particles). Here, we should point out that electrons in the oxygen vacancy defects might contribute to the optical emission process through Förster energy transfer [25]. This is understandable, since the oxygen vacancy defects are distributed over all the alumina particles which conform to the action range of Förster energy transfer. Also, we can see from the diagram that the energy levels of defects overlap with the modified energy levels (conduction band and valence band) of alumina particles. According to the quantum confinement effect, smaller particles have wider bandgaps and thereby larger optical emission energies. This explains why the PL is shifted to blue in the stored samples (B and C), since larger particles precipitate with time. This conjecture also explains why there are much smaller blueshifts between samples A, B and C under excitation with the 370 nm line compared with the 330 nm line. On the other hand, under lower excitation energies smaller particles cannot be excited; this leads to a more concentrated size distribution of excitable particles and thus results in weaker blueshifts between samples A, B and C. This agrees with our PL results. As noted above, the emission band widths at half maximum are greater under excitation of 330 nm with respect to 370 nm. This is because one wide emission curve is composed of many narrow emission curves of particles with different sizes, so the PL curve is wider for higher excitation energy since more particles could be excited. Also, the precipitation of partial alumina particles will lead to the decrease of emission intensity with time (see figure 1(a)). Finally, as no interaction has been reported between the alumina surface and the chloroform solvent, no obvious shift in PL is observed in figure 1(b), which further confirms our assumed optical emission level combining the surface bonding states with the energy levels of alumina modified by the quantum confinement effect.

In summary, we have fabricated amorphous alumina nanoparticles suspended in toluene. The PL is shifted to blue as the particle sizes decrease, while the PLE spectrum exhibits a wide absorption band. A model based on the modified energy levels of alumina particles explains well the observed PL spectra. The surface bonding energy levels and the oxygen defect levels are considered to be responsible for the wide absorption band in PLE. Our work indicates that the luminescence of alumina nanoparticles could help to investigate the band structures and the luminescent centres of amorphous alumina, and provides an experimental basis for theoretical study.

Acknowledgments

This work was supported by grants (Nos 10225416 and BK2006715) from the National and Jiangsu Natural Science Foundations and the LAPEM. Partial support was also provided by the Major State Basic Research Project No G001CB3095 of China and City University of Hong Kong Direct Allocation Grant No 9360110.

References

- [1] Folser F 1994 *Appl. Phys. A* **59** 209
- [2] Hench L L 1991 *J. Am. Ceram. Soc.* **74** 1487
- [3] Keller A R and Zhou M 2003 *J. Am. Ceram. Soc.* **86** 449
- [4] Keller F, Hunter M S and Robinson D L 1953 *J. Electrochem. Soc.* **100** 411
- [5] Yamamoto Y, Baba N and Tajima S 1981 *Nature* **289** 572
- [6] Furneaux R C, Rigby W R and Davidson A P 1989 *Nature* **337** 147
- [7] Masuda H and Fukuda K 1995 *Science* **268** 1466
- [8] Li A P, Müller F, Birner A, Nielsch K and Gösele U 1998 *J. Appl. Phys.* **84** 6023
- [9] Jessensky O, Müller F and Gösele U 1998 *Appl. Phys. Lett.* **72** 1173
- [10] Bao J C, Tie C Y, Xu Z, Zhou Q F, Shen D and Ma Q 2001 *Adv. Mater.* **13** 1631
- [11] Sander M S and Tan L S 2003 *Adv. Funct. Mater.* **13** 393
- [12] Li J, Papadopoulos C and Xu J M 1999 *Nature* **402** 253
- [13] Wu G S, Zhang L D, Cheng B C, Xie T and Yuan X Y 2004 *J. Am. Chem. Soc.* **126** 5976
- [14] Jeong S H, Cha Y K, Yoo I K, Song Y S and Chung C W 2004 *Chem. Mater.* **16** 1612
- [15] Hoyer P, Baba N and Masuda H 1995 *Appl. Phys. Lett.* **66** 2700
- [16] Huang G S, Wu X L, Mei Y F, Shao X F and Siu G G 2003 *J. Appl. Phys.* **93** 582
- [17] Qiu T, Wu X L, Kong F, Ma H B and Chu P K 2004 *Phys. Lett. A* **334** 447
- [18] Huang G S, Xie Y, Wu X L, Yang L W, Shi Y, Siu G G and Chu P K 2006 *J. Cryst. Growth* **289** 295
- [19] Du Y, Cai W L, Mo C M, Chen J, Zhang L D and Zhu X G 1999 *Appl. Phys. Lett.* **74** 2951
- [20] Li Y, Li G H, Meng G W, Zhang L D and Phillipp F 2001 *J. Phys.: Condens. Matter* **13** 2691
- [21] Qi D, Kwong K, Rademacher K, Wolf M O and Young J F 2003 *Nano Lett.* **3** 1265
- [22] van der Beek G P, Stuart M A C, Fleer G J and Hofman J E 1991 *Macromolecules* **24** 6600
- [23] Nagao M and Suda Y 1989 *Langmuir* **5** 42
- [24] Wu X L, Qiu T, Hu D S, Huang G S, Yuan R K, Siu G G and Chu Paul K 2006 *J. Chem. Phys.* **125** 054713
- [25] Huang G S, Wu X L, Xie Y, Kong F, Zhang Z Y, Siu G G and Chu P K 2005 *Appl. Phys. Lett.* **87** 151910